Theoretical Study of the Gas-Phase Reaction of Fluoride and Chloride Ions with Methyl Formate

Josefredo R. Pliego, Jr.[†] and José M. Riveros*

Instituto de Química, Universidade de São Paulo, Caixa Postal 26077, CEP 05513-970 São Paulo, SP, Brazil

Received: April 16, 2001; In Final Form: October 17, 2001

The potential energy surface of the gas-phase reaction between halide ions (F^- and Cl^-) and methyl formate has been investigated by ab initio calculations. For F^-, two pathways have been observed at thermal energies and identified in the calculations: (1) α-elimination of CO to yield a fluoride−methanol adduct, the so-called Riveros reaction that has found wide application in gas-phase ion chemistry, and (2) S_N2 displacement of $HCOO^-$. The first reaction is shown to proceed by the initial formation of a loose complex followed by formal abstraction of a formyl hydrogen to yield a three-body complex that dissociates into the final products. The S_N2 reaction initially involves formation of a loose complex with the fluoride attached to the methyl group of the ester. The first pathway is calculated to go through a lower energy local transition state than the corresponding S_N2 reaction but the transition states are located below the energy of the reagents. Both ion−neutral complexes can interconvert via formation of a stable tetrahedral intermediate. The product distribution was estimated via a simple RRKM calculation that predicts 92% of α-elimination and 8% of S_N2 reaction. This prediction is in excellent agreement with measurements carried out by FT-ICR. This product distribution is predicted to remain essentially unchanged for the reaction with $DCOOCH_3$ in agreement with experimental observations. A similar analysis of the corresponding $Cl^- + HCOOCH_3$ reaction reveals that α-elimination has a substantial activation energy (well above the reagents) accounting for the failure to observe this reaction even though it is exothermic. These calculations also reveal that for the Cl^- system, the tetrahedral intermediate is not a stable intermediate in agreement with previous experimental data on related systems.

Introduction

Gas-phase ion chemistry, and particularly the study of ion−molecule reactions, have significantly furthered our understanding of intrinsic reactivity and helped to unravel the mechanism of chemical reactions under solvent-free conditions.[1] This is best exemplified by gas-phase nucleophilic displacement (S_N2) reactions where a lively interplay between experiment and theory has contributed to the elucidation of the energetics, the potential energy surface, and the dynamics of these reactions.[2−4] Because of their relevance to many important organic and biochemical processes gas-phase reactions between esters and anionic nucleophiles have also been the subject of a large number of experimental studies.[5] However, considerably less is known about the potential energy surface and the dynamics for these systems since several mechanisms leading to different products are operative even for the simplest cases.

Experiments from our laboratories[6,7] as well as work from other groups[5d,5f,8,9] have revealed that the reaction of ions such as OH^-, F^-, RO^- (R = alkyl), and NH_2^-, with methyl formate can proceed by α-elimination of CO, S_N2 displacement at the methyl group, and/or addition−elimination at the carbonyl center as illustrated in Scheme 1 (X^- = nucleophile).

While the product distribution is dependent on the thermochemistry and the nature of the nucleophile, reaction 1a is the preferred pathway for ions such as F^-, OH^-, and RO^-. As a result, reaction 1a has become well established in gas-phase ion chemistry[10] and has been routinely used as a convenient method to generate gas-phase mono-solvated anions[11] in experiments designed to determine binding energies,[12] structure,[13] and spectroscopic characterization.[14] On the other hand, it is still unclear as to why reaction 1a is not observed for second-row anions such as Cl^- although the reaction is exothermic.

SCHEME 1

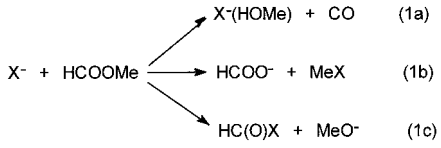

Given the ease of reaction 1a for simple nucleophiles, the question arises regarding the nature of the potential energy surface that favors such a pathway as opposed to the traditional viewpoint of nucleophilic attack at the carbonyl system. We have recently addressed this particular question for the reaction of OH^- vis-à-vis the gas-phase hydrolysis reaction 1b that can proceed either by a $B_{AC}2$ or an S_N2 mechanism.[15] At the highest level of theory reported in our earlier work (MP4/6-311+G(2df,2p)//MP2/6-31+G(d)), reaction 1a was found to proceed by abstraction of the formyl proton and formation of a three-body complex, $CH_3O^-(H_2O)(CO)$ without any formal activation energy along the reaction pathway. In this report, we extend our ab initio calculations to the F^- and Cl^- reactions in order to understand two important features: (a) the strong preference for reaction 1a over the competing S_N2 reaction 1b for F^-; (b) the lack of any reactivity for Cl^-.

* Author to whom correspondence should be addressed at Instituto de Química, University of São Paulo, Caixa Postal 26077, São Paulo, Brazil, CEP 05513-970. Phone/Fax: 55-11-3818-3888. E-mail: jmrnigra@iq.usp.br.

[†] E-mail: josef@iq.usp.br.

10.1021/jp0114081 CCC: $22.00
Published on Web 12/20/2001

Failure to observe a reaction between Cl^- and $HCOOCH_3$ was originally rationalized in terms of the thermochemistry involved in the association of anions with methanol and the energy required to decarbonylate methyl formate.[16] Unfortunately, this argument cannot explain the origin of a possible energy barrier for the case of Cl^-. Our present calculations for the energy surface profile of the F^- reaction coupled with statistical rate theories yield excellent agreement with the experimentally observed product distribution. Likewise, these calculations reveal a substantial energy barrier for reaction 1a when Cl^- is the nucleophile. Thus, it is possible to have a unified view about this useful and common reaction in the gas phase.

Experimental Section

A recent study[5f] of the gas-phase $F^- + HCOOCH_3$ reaction showing a considerably different product distribution from our earlier experiments[7] prompted us to reexamine this system in our FT-ICR spectrometer. The general features of this spectrometer have been discussed in recent publications from this laboratory.[17] The temperature of the cell is typically around 330 K while the magnetic field was maintained at 1.0 T.

Fluoride ions were generated directly in the cell of the spectrometer by electron impact at 3.4 eV from NF_3 at a nominal pressure of 1.8×10^{-8} Torr. For a typical 80 ms ionization pulse, an electron ejection pulse of 150 ms was applied to the trapping plates with the radio frequency field tuned to ~7.5 MHz. The electron ejection pulse is essential for reducing space charge effects due to trapped thermal electrons. Methyl formate (Aldrich) was introduced in the spectrometer at a pressure of 7.5×10^{-9} Torr, and its pressure was periodically remeasured after pumping away NF_3. Nitrogen was added to the system up to a total pressure of 2×10^{-7} Torr in order to help the thermalization of the reagent ions. In a different set of experiments, nitrogen was introduced through a pulsed valve to achieve a maximum instantaneous pressure of 5×10^{-7} Torr. Ion/molecule reactions were studied by isolating fluoride ions in the reaction cell through a sequence of short pulses to remove all other ions at times ranging from 500 to 2500 ms after ion formation. The reaction products of the $F^-/HCOOCH_3$ system were determined from FT-ICR spectra typically recorded with 32 K data at different reaction times. While no attempt was made to measure the absolute rate constants in these experiments due to the uncertainties in the value of the absolute pressures, the product distribution was determined from the relative peak intensities of the magnitude spectra of the product ions[18] acquired with impulse excitation.[19] Impulse excitation is routinely used in our laboratory because at low ion densities it yields excellent isotopic ratios as frequently verified in our spectrometer with germanium-containing ions.[17d] The advantage of impulse excitation in these cases resides in the fact that all ions in the cell are accelerated simultaneously to the same large radius of gyration in a short period of time thus minimizing some of the problems associated with mass discrimination in FT-ICR spectra.[20,21]

F^- reacts with $HCOOCH_3$ along two different pathways as shown in reaction 2 along with the product distribution. These

		$HCOOCH_3$	$DCOOCH_3$	
$F^- + HCOOCH_3$ →	$F^-(HOCH_3) + CO$	0.92 ± 0.015	0.90 ± 0.015	(2a)
→	$HCOO^- + CH_3F$	0.08 ± 0.015	0.10 ± 0.015	(2b)

results represent the average of 10 independent measurements and were found to be independent of reaction time within experimental error. Similar experiments were also carried out with 99% $DCOOCH_3$ and the product distribution is observed to be essentially unchanged upon deuteriation at the formyl hydrogen (see Figure 1). These results are in excellent agreement with those reported in our previous work.[7]Experiments carried out with a 10-fold, or higher, increase in the pressure of methyl formate reveal that $F^-(HOCH_3)$ ions can undergo a slow reaction similar to reaction 2a to yield $F^-(CH_3OH)_2$ ions. This kind of sequential "Riveros reaction" initiated by a mono-solvated anion has already been observed for alkoxide ions,[22] and for CF_3^-.[12c]

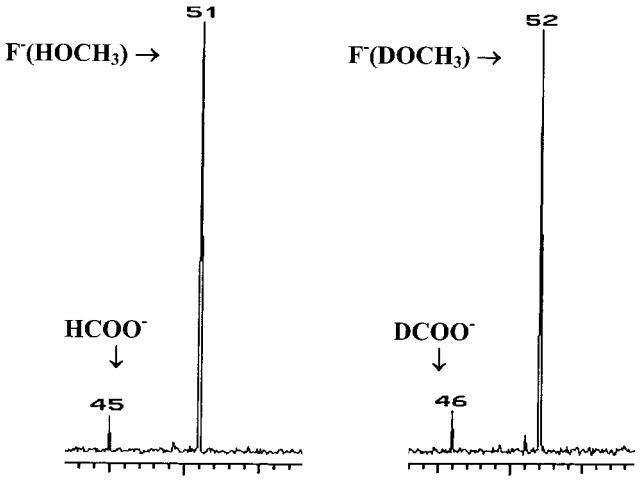

Figure 1. FT-ICR spectra of the products of reaction 2. The left-hand side shows the product distribution for the $F^-/HCOOCH_3$ reaction and the right side the corresponding product distribution for the $F^-/DCOOCH_3$ reaction.

Ab Initio Calculations. The potential energy surface for the gas-phase reaction of X^- (X = F, Cl) with $HCOOCH_3$ was initially explored at the MP2 level of theory using the standard 6-31+G* basis set. This level of calculation was used to locate the structures corresponding to local minima and transition states. All stationary points were characterized by harmonic frequency analysis, and the frequencies were used to determine zero-point vibrational energies (ZPE) without any scaling procedure. For the $F^- + HCOOCH_3$ system, higher-level single-point calculations at the MP2/6-311+G(2df,2p) and MP4/6-31+G* levels were performed in conjunction with an additivity approximation to obtain effective MP4/6-311+G(2df,2p) energies. Comparison of the most significant results obtained by this methodology with those derived from calculations carried out with full MP4/6-311+G(2df,2p) energies reveal very good agreement and are discussed later in this paper.

For the $Cl^- + HCOOCH_3$ system we have only used the MP2/6-31+G* energies since the relatively high barriers encountered for this system precluded an investigation at a higher level of theory for reasons explained in the discussion. All ab initio calculations were done with the Gaussian 94 suite of programs.[23]

The $F^- + HCOOCH_3$ System. Figure 2 outlines the detailed mechanisms of the reactions that were characterized in this work for the $F^- + HCOOCH_3$ system. Each step of the mechanism as well as intermediates and transition states has been numerically labeled for convenience. The optimized structures for all minima and transition states encountered for the different pathways are shown in Figures 3 and 4, while Table 1 lists the reaction and activation energies for each step. A graphical representation of the potential energy surface profile is shown in Figure 5.

Minima and Transition State Structures. The interaction of F^- with methyl formate leads to the formation of two ion−

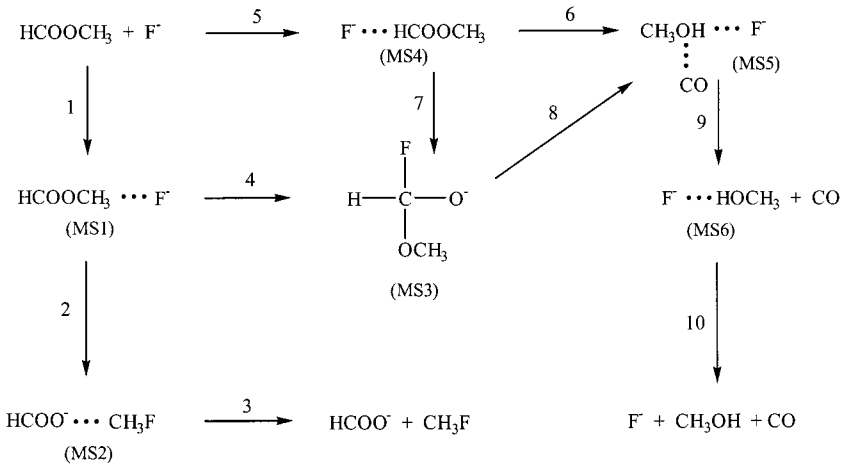

Figure 2. A general diagram of the reaction pathways for the gas-phase F^- + $HCOOCH_3$ system.

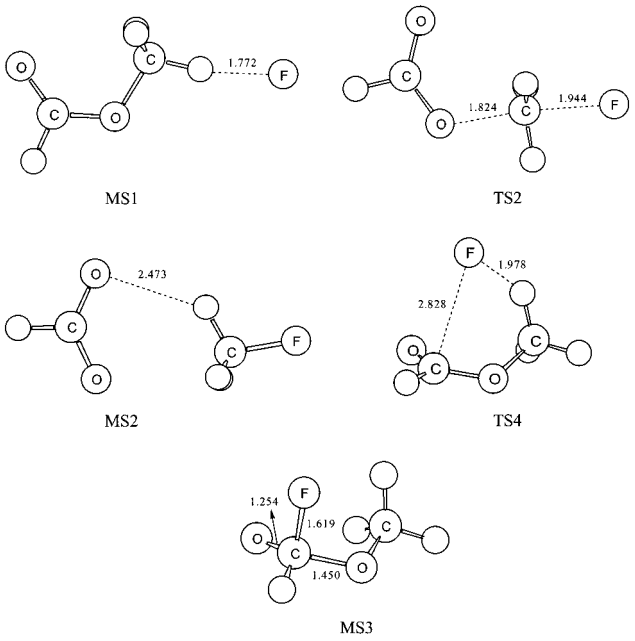

Figure 3. Structure of intermediates and transition states resulting from the initial formation of the S_N2 entrance complex (MS1) leading to the S_N2 reaction and to formation of the tetrahedral species (MS3).

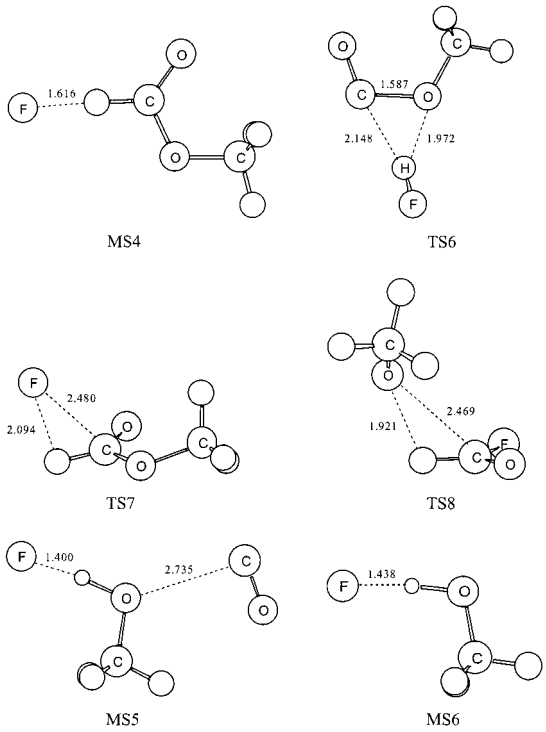

Figure 4. Structure of intermediates and transition states resulting from abstraction of the formyl hydrogen by the fluoride ion.

molecule complexes labeled MS1 and MS4 in Figures 2−5. The MS1 complex can undergo an S_N2-type displacement through transition state TS2 that leads to the MS2 exit complex of the well-established S_N2 double well potential.[2] This complex can then dissociate to the final products, i.e., $HCOO^-$ and methyl fluoride. While passage of the MS1 to the MS2 complex is calculated to involve a barrier of 9.0 kcal mol^{-1}, this transition state (TS2) is still well below the energy of the reagents. The calculated exothermicity for the S_N2 reaction amounts to 23.7 kcal mol^{-1} in close agreement with a value of 21.5 ± 3 kcal mol^{-1}derived from available experimental data.[24] The MS1 complex can also proceed to form a tetrahedral intermediate (MS3 structure) through transition state TS4, and the barrier for this step is calculated to be only 4.1 kcal mol^{-1}. This pathway is similar to that found for the gas-phase reaction of OH^-.[15,25] While the MS3 tetrahedral intermediate can undergo methanol elimination through step 8 to yield the MS5 complex, this step involves a barrier of 21.4 kcal mol^{-1} with the TS8 structure calculated to be 2.1 kcal mol^{-1} *above* the energy of the reactants (see Figure 5).

By comparison, the MS4 ion−neutral complex can proceed either through steps 6 or 7 (Figures 2 and 5). Step 7 leads to the formation of the tetrahedral intermediate through transition state TS7 located 6.9 kcal mol^{-1} above the energy of the complex but 13.9 kcal mol^{-1} *below* the energy of the reagents. The fate of this tetrahedral intermediate was discussed above and further reaction is expected to be unfavorable on the basis of our calculations. The other pathways, step 6, leads to the proton abstraction of the formyl proton and formation of the three-body MS5 complex. Unlike the energy surface calculated for the similar OH^- reaction,[15] step 6 has a substantial energy barrier amounting to 11.2 kcal mol^{-1} at our best level of calculation.[26] The three-body MS5 complex is characterized by a very low binding energy (3.6 kcal mol^{-1}) with respect to the ultimate products of reaction 2a, namely the fluoride−methanol adduct, MS6, and CO. The binding energy of the fluoride−methanol is calculated to be 30.1 kcal mol^{-1}, in excellent agreement with the experimental[12a] binding enthalpy of 29.6 ±

TABLE 1: Reaction and Activation Energies for the Reaction Pathways of $F^- + HCOOCH_3$[a]

Reaction Energies

step	MP2/6-31+G(d)	MP2/6-311+G(2df,2p)	MP4/6-31+G(d)	MP4/6-311+G(2df,2p)[b]	ΔZPE[c]	Δ*E*
1	−15.81	−17.73	−16.11	−18.04	0.23	−17.81
2	−13.67	−15.45	−13.59	−15.37	−1.13	−16.50
3	11.50	11.07	11.82	11.39	−0.73	10.66
4	0.68	−1.69	0.57	−1.80	0.34	−1.46
5	−17.75	−20.14	−18.22	−20.61	−0.19	−20.80
6	1.42	0.77	−0.19	−0.84	−3.25	−4.09
7	2.63	0.72	2.68	0.77	0.76	1.53
8	−1.21	0.05	−2.87	−1.61	−4.01	−5.62
9	3.72	3.59	4.08	3.94	−0.34	3.61
10	28.56	30.77	27.97	30.18	−0.13	30.05

Activation Energies

step	MP2/6-31+G(d)	MP2/6-311+G(2df,2p)	MP4/6-31+G(d)	MP4/6-311+G(2df,2p)[b]	ΔZPE‡	Δ*E*‡
2	11.75	12.00	9.81	10.07	−1.08	8.99
4	4.54	4.54	4.14	4.15	−0.06	4.09
6	20.04	15.41	19.04	14.42	−3.09	11.33
7	6.76	6.95	6.36	6.55	0.36	6.91
8	27.77	25.05	27.14	24.42	−3.06	21.36

[a] Energies in units of kcal mol^{-1}; steps numbered according to Figure 2. [b] Obtained by additivity approximation. [c] Zero-point vibrational energy contribution.

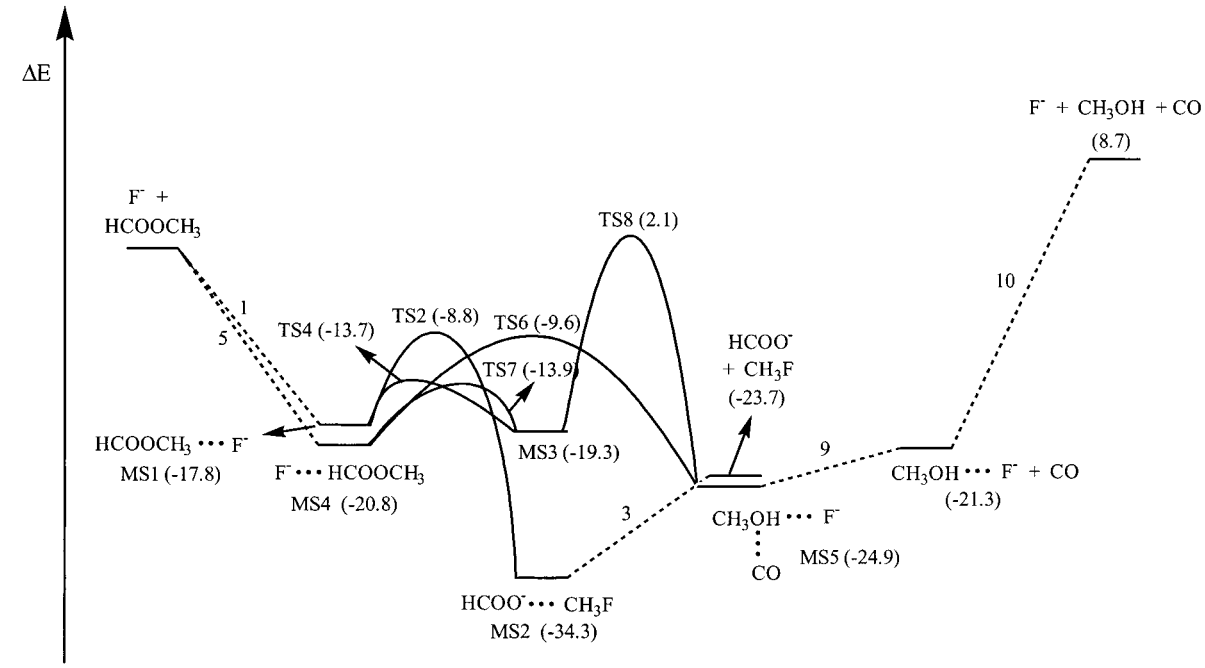

Figure 5. Calculated potential energy profile for the gas-phase $F^- + HCOOCH_3$ reaction.

2 kcal mol^{-1} and a value of 30.4 kcal mol^{-1} calculated previously at the CCSD level with a large basis set.[27]

Analysis of the Reaction Paths. The potential energy surface profile displayed in Figure 5 and discussed above is qualitatively consistent with the experimental results and with the nature of the reaction products in reaction 2. According to this profile, collisions between F^- ions and methyl formate lead to the formation of MS1 and MS4 ion−molecule complexes. Both of these species can form the tetrahedral intermediate MS3 through TS4 or TS7, representing barriers of relatively low activation barriers when compared with the energy content of the system. However, this tetrahedral intermediate is unlikely to lead to reaction products since TS8 involves a high barrier as discussed above. However, this tetrahedral intermediate provides a communication channel between the MS1 and MS4 complex. Since ion−molecule reactions typically proceed through long-lived intermediates, it is possible to assume an equilibrium distribution between the MS1, MS3, and MS4 complexes (with the MS4 complex being the predominant one) and the final products to be formed through TS2 and TS6.

The efficiency of the S_N2 reaction is thus expected to depend on the probability of passing through TS2 since the MS2 complex would be formed with enough energy for dissociation to the $HCOO^- + CH_3F$ products. By comparison, the efficiency of the decarbonylation reaction will be dictated by the probability of passing through TS6, a pathway with a lower activation barrier than TS2. The final products are then expected to be $CH_3OH\cdots F^- + CO$ as a result of dissociation of the energy-rich MS5 complexes.

RRKM Calculations. The expected product distribution for reaction 2 can be estimated from a microcanonical analysis of the unimolecular rate constants for the intermediate complex. This approach assumes that the system displays statistical behavior, a reasonable starting point in the absence of any

TABLE 2: Harmonic Vibrational Frequencies for the Structures MS4, TS2, and TS6[a]

MS4	TS2	TS6
108	60	53
109	124	77
170	177	170
232	333	195
331	357	262
415	370	294
749	770	532
933	1049	728
1119	1128	799
1188	1162	1037
1224	1243	1175
1242	1348	1180
1491	1426	1469
1505	1437	1524
1530	1440	1547
1551	1700	1688
1687	2948	3033
2582	3238	3094
3097	3440	3135
3179	3444	3505
3211	-	-

[a] Units of cm^{-1}. Values obtained at MP2/6-31+G(d) level of theory.

experimental data to the contrary. We have previously used this kind of approach in the analysis of the product distribution of the $OH^- + HCOOCH_3$ reaction and the theoretical predictions were found to be in excellent agreement with experimental observations.[15] Thus, a simple RRKM approach was also used in the present case to estimate the product distribution for the $F^-/HCOOCH_3$ system.

The analysis is based on the assumption that equilibrium between the MS1, MS3, and MS4 species is faster than the lifetime of these intermediate species. Under these conditions, we can take the MS4 complex, the most stable, as the reference species and compute the reaction rate constants through TS2 and TS6 by RRKM theory. For the sake of simplicity rotational effects have not been considered ($J = 0$), and the internal energy available (E^*) to the MS4 complex is then calculated by the following equation:

$$E^* = \Delta E_{MS4} + E_R - E_{MS4}$$

where ΔE_{MS4} is the energy released upon formation of the MS4 complex (20.80 kcal mol^{-1}), E_R is the thermal contribution to the translational, rotational, and vibrational energy of the reactants (3.70 kcal mol^{-1}), and E_{MS4} is the thermal contribution to the translational and rotational energy of the MS4 complex (1.78 kcal mol^{-1}). Thus, at 298 K the energy available to the MS4 species is $E^* = 22.7$ kcal mol^{-1}. The barrier heights for TS2 and TS6 are 12.0 kcal mol^{-1} and 11.3 kcal mol^{-1}, respectively, and the calculated harmonic vibrational frequencies are listed in Table 2.

RRKM calculations were then performed using the Zhu and Hase program,[28] and the resulting unimolecular rate constants ($k_{TS2} = 4.70 \times 10^{10}$ s^{-1} and $k_{TS6} = 5.08 \times 10^{11}$ s^{-1}) yield the following branching ratio for reaction 2: 92% decarbonylation (the Riveros reaction 2a) and 8% for the S_N2 path (reaction 2b). This result is in very good agreement with our previous measurements[7] and with those reported in the present set of experiments. Furthermore, this branching ratio remains essentially unchanged with increasing internal energy of the reagents as verified by RRKM calculations carried out with higher values of E^*.[29] This prediction also agrees with the experiments that show no significant variation with the thermalization time of the ions.

TABLE 3: Single-Point Calculations at Exact MP4/6-311+G(2df,2p) and MP2/6-311+G(2df,2p) Levels and Using Additivity Approximation for the MP4 Method[a]

process	MP4 (exact)	MP4 (additivity)[b]	MP2
MS4 → TS2	12.38	12.64	14.41
MS4 → TS6	14.03	14.42	15.41
TS2 → TS6	1.65	1.78	1.00

[a] In kcal mol^{-1}. [b] In the additivity approximation E[MP4/6-311+G(2df,2p)] ≈ E[MP4/6-31+G(d)] + E[MP2/6-311+G(2df,2p)] − E[MP2/6-31+G(d)].

A similar RRKM calculation was also carried out for the $F^- + DCOOCH_3$ reaction by using the calculated vibrational frequencies of the deuterium-substituted MS4 and the corresponding transition state structures. The resulting unimolecular rate constants, $k_{TS2}(DCOOCH_3) = 4.0 \times 10^{10}$ s^{-1} and $k_{TS6}(DCOOCH_3) = 3.9 \times 10^{11}$ s^{-1}, predict for $DCOOCH_3$ a branching ratio of 91% for the decarbonylation path (the Riveros reaction 2a) and 9% for the S_N2 path (reaction 2b). This small change in branching ratio upon deuteriation at the formyl position is also in excellent agreement with the present experimental findings.

Due to the importance of the local energy barriers in the overall energy surface and the barrier heights in determining the calculated branching ratio, we have tested the accuracy of our additivity approximation by performing exact MP4/6-311+G(2df, 2p) single-point calculations on the key structures, namely MS4, TS2, and TS6. Table 3 lists the barriers for the MS4 → TS2 and MS4 → TS6 processes, as well as the energy variation involved in going from TS2 to TS6, calculated at the MP4/6-311+G(2df,2p) level, at the MP2/6-311+G(2df,2p) level, and using the additivity approximation. The results shown in Table 3 clearly point out that the additivity approximation is indeed very adequate with barrier heights that are predicted to be different by less than 0.4 kcal mol^{-1} with those calculated at the exact MP4/6-311+G(2df,2p) level. By comparison, barrier heights calculated at the MP2/6-311+G(2df,2p) level differ as much as 2 kcal mol^{-1} from those calculated at higher levels of theory. Even more important and critical to the calculation of the branching ratio is the calculated variation in energy in going from TS2 to TS6 structure (TS2 → TS6). The additivity approximation yields a value that is only 0.13 kcal mol^{-1} different from that obtained at the full MP4 calculation, while the MP2 calculation yields a value that differs by 0.65 kcal mol^{-1}. These results clearly point out that the additivity approximation used in our work is capable of predicting a potential energy surface in very close agreement with that obtained at the exact MP4 level and at a considerable savings of computational time. Thus, very small differences in the calculated branching ratio would result from using the values obtained by the exact MP4 calculation or by additivity approximation. On the other hand, the MP2 calculations would lead to a considerably less reliable potential energy surface and branching ratio.

The $Cl^- + HCOOCH_3$ System. The fact that reaction 1a is not observed with Cl^- led us to analyze the profile of the potential energy surface in a fashion similar to that described above. The available experimental data[20] predicts the Cl^--promoted S_N2 reaction (reaction 1b in Scheme 1) to be endothermic by 9 ± 3 kcal mol^{-1}. Thus, the fact that no $HCOO^-$ displacement is observed in the ion−molecule reaction of Cl^- with $HCOOCH_3$ can be readily understood on thermochemical grounds. On the other hand, similar experimental data[30] predict the so-called Riveros (reaction 1a) to be *exothermic* by 6 ± 2 kcal mol^{-1}.

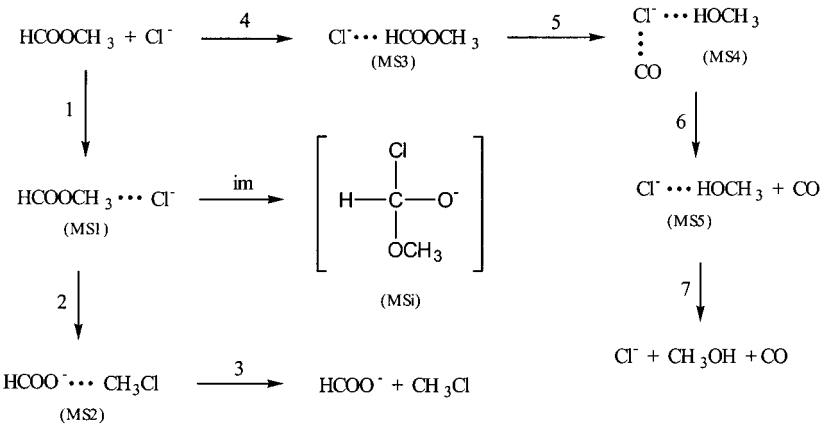

Figure 6. A general diagram of the reaction pathways for the gas-phase $Cl^- + HCOOCH_3$ system.

TABLE 4: Reaction and Activation Energies for the Gas-Phase Reaction $Cl^- + HCOOCH_3$[a]

Reaction Energies

step	MP2/6-31+G*	ΔZPE[b]	Δ*E*
1	−9.67	0.29	−9.38
2	6.91	−2.13	4.78
3	11.97	−0.65	11.32
4	−9.30	0.32	−8.98
5	5.52	−2.89	2.63
6	3.58	−0.56	3.03
7	16.16	−0.78	15.38
im	32.41	0.00	32.41

Activation Energies

step	MP2/6-31+G*	ΔZPE‡	Δ*E*‡
2	22.69	−1.82	20.87
5	49.53	−5.56	43.97

[a] Energies in units of kcal mol^{-1}; steps numbered according to Figure 6. [b] Zero-point vibrational energy contribution.

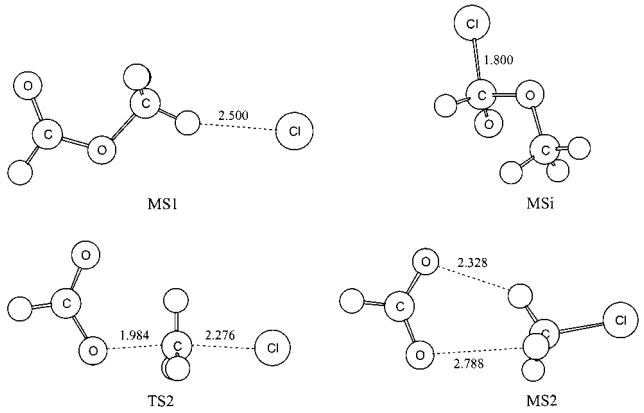

Figure 7. Structure of intermediates and transition states resulting from attachment of the chloride ion to the methyl group of the ester.

Our theoretical results for this system are shown in Figures 6 to 9 and are summarized in Table 4. Figure 6 outlines the reaction pathways investigated by analogy with the F^- reactions, and Figures 7 and 8 display the optimized structures for the local minima and transition states. The calculated potential energy surface profile is represented in Figure 9.

Analysis of the Potential Energy Surface. As in the case of the fluoride ion, the interaction of the Cl^- ion with methyl formate leads to two possible ion−molecule complexes, namely MS1 and MS3. These are calculated to have stabilization energies close to 9 kcal mol^{-1}. The S_N2 mechanism for the reactant side MS1 complex is predicted to have a substantial

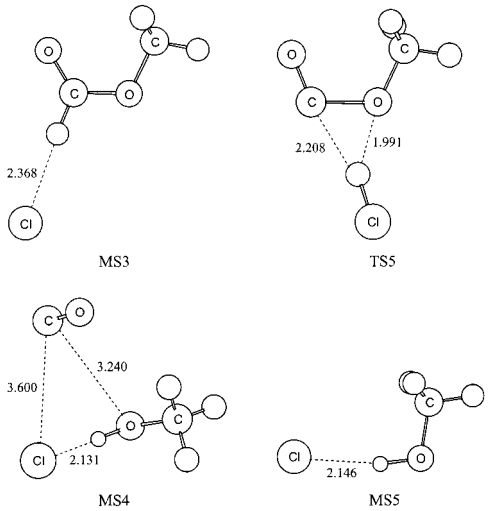

Figure 8. Structure of intermediates and transition states resulting from abstraction of the formyl hydrogen by the chloride ion. The MSi species is a putative tetrahedral intermediate that is not a minimum in the potential energy surface (see text).

activation energy and the TS2 structure is located 11.5 kcal mol^{-1} above the reagents. Thus, passage to the exit MS2 complex, located 4.6 kcal mol^{-1} below the energy of the reagents, and dissociation of MS2 to $HCOO^-$ and methyl chloride is highly unfavorable at thermal energies. The overall endothermicity of the S_N2 reaction is predicted to be 6.7 kcal mol^{-1} at the MP2/6-31+G* level of theory.

The decarbonylation mechanism involving the MS3 complex was found to have a very high activation energy associated with the TS5 structure, located 35 kcal mol^{-1} above the energy of the reagents! This barrier allows us to conclude that no reaction is expected to be observed by techniques such as ion-cyclotron resonance or flowing afterglow even though the overall reaction is exothermic. The potential energy surface for this pathway also reveals the three-body product side complex, MS4 in Figure 9, that is located 6.4 kcal mol^{-1} below the energy of the reagents. If this species were to be formed, it would then lead to loss of CO and formation of the $CH_3OH\cdots Cl^-$ adduct.

Another possibility that we have investigated is formation of a tetrahedral intermediate as encountered for the F^- ion. In this case, the tetrahedral species is found not to be minimum on the potential energy surface. To estimate the stability of a hypothetical tetrahedral like structure for this system, a calculation was performed with the C−Cl distance frozen at 1.8 Å, and optimizing the remaining geometrical parameters. This is

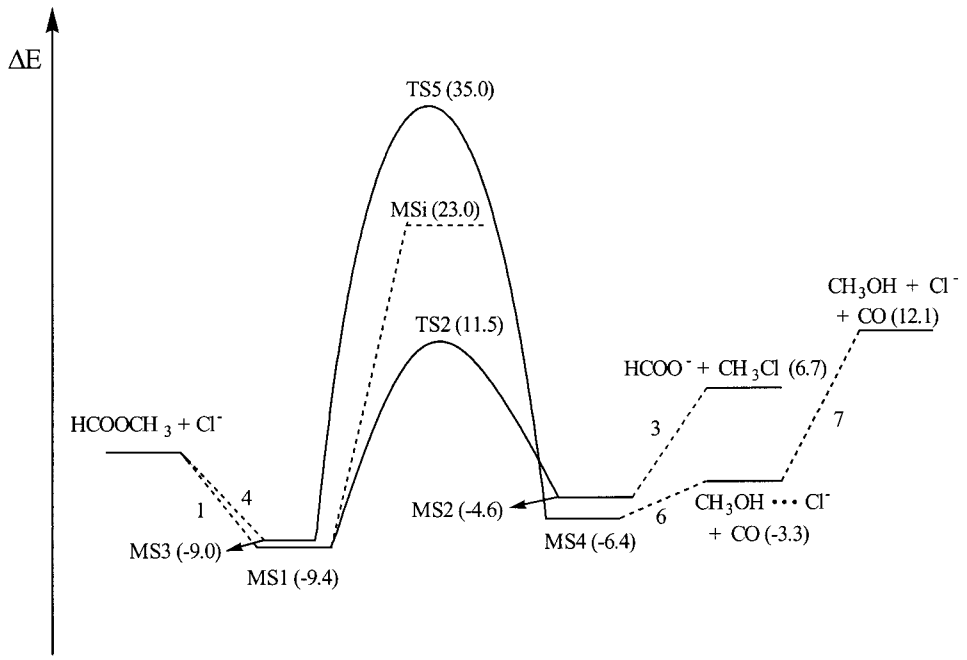

Figure 9. Calculated potential energy profile for the gas-phase $Cl^- + HCOOCH_3$ reaction.

represented by the MSi structure located 23.0 kcal mol^{-1} above the energy of the initial reagents.

This energy surface profile clearly predicts that both channels are energetically unfavorable and are consistent with the experimental results that show no reactivity for this system.[16]

The fact that the barrier for the decarbonylation reaction was found to be very high precluded the need for calculations at higher levels of theory. On the basis of the more extended calculations for the $F^-/HCOOCH_3$ system, we can in fact estimate that the barrier predicted by our MP2/6-31+G(d) calculation for the $Cl^-/HCOOCH_3$ reaction could probably be in error by 2 or 3 kcal mol^{-1} at most. Even with this uncertainty, the transition structure TS5 would still lie considerably above the energy of the reagents, and no reaction is expected to be observed within the conventional time and pressure regimes of gas-phase ion chemistry techniques.

Discussion

The potential energy surface for the gas-phase reaction of anionic nucleophiles with methyl formate, discussed in this paper and in ref 15, reveals the formation of a highly favorable complex with the anion bound to the formyl hydrogen of the ester. Our calculations show that the barrier associated with further abstraction of this proton and the subsequent formation of an anion−methanol adduct and CO scales with the basicity of the corresponding nucleophile. In fact, these studies clearly show the barrier to increase in the order OH^- (no barrier)[15] < $F^- \ll Cl^-$, with the last case involving an energy barrier well above that of the reagents. A second reaction complex that can also be formed in these systems is that corresponding to the S_N2 entrance complex.[31] The activation energy calculated for these complexes to proceed to $HCOO^-$ and MeX (X^- = nucleophile) also follows the same trend with $OH^- < F^- \ll Cl^-$, although in the latter case the overall reaction is endothermic.

A second important aspect is the question of nucleophilic attack at the carbonyl center and formation of a tetrahedral species in a simple ester such as methyl formate. For OH^- and F^-, the potential energy surface clearly shows that formation of a stable tetrahedral intermediate in these cases stems from the complexes discussed above, and not as a direct process. For the Cl^- ion, the tetrahedral species of methyl formate is not a stable intermediate but a transition state, a result that is of considerable significance. An earlier theoretical study of the thermoneutral chloride displacement reaction between Cl^- and either formyl chloride, HCOCl, or acetyl chloride, CH_3COCl, predicted the tetrahedral structures to be transition states for these reactions rather than stable intermediates.[32] These findings are consistent with experimental observations that the chlorines are not equivalent in the ion−neutral complexes of Cl^- with CH_3COCl and CH_3OCOCl, and thus these complexes are best described as ion−dipole complexes rather than tetrahedral intermediates.[33]

Finally, we have made use of a very simple approach to estimate the product distribution in these systems. This approach, based on RRKM theory, predicts branching ratios that are in excellent agreement with experimental findings.

The significant changes in the potential energy surface for equivalent reactions in solution is presently being investigated in order to learn how solvent effects can extensively modify intrinsic reactivity and the outcome of well-known chemical reactions.

Acknowledgment. This work was made possible by the support of a grant and a postdoctoral fellowship (J.R.P.) from the São Paulo Science Foundation (FAPESP), and a Senior Research fellowship from the Brazilian Research Council (C.N.Pq). The authors also acknowledge the help of Gustavo H. Guedes (undergraduate FAPESP scholarship) with some of the experiments.

References and Notes

(1) For two recent reviews, see (a) Gronert, S. *Chem. Rev.* **2001**, *101*, 329. (b) DePuy, C. H. *Int. J. Mass Spectrom.* **2000**, *200*, 79.

(2) For a general discussion of potential energy surfaces for these reactions, see Chabinyc, M. L.; Craig, S. L.; Regan, C. K.; Brauman, J. I. *Science* **1998**, *279*, 1882, and references therein.

(3) For a benchmark large-scale coupled cluster calculation for the F^- + CH_3Cl reaction, see Botschwina, P.; Horn, M.; Seeger, S.; Oswald, R. *Ber. Bunsen-Ges. Phys. Chem.* **1997**, *101*, 387.

(4) Hase, W. L. *Science* **1994**, *266*, 998.

(5) (a) Jose, S. M.; Riveros, J. M. *Nouveau J. Chim.* **1977**, *1*, 113. (b) Takashima, K.; Riveros, J. M. *J. Am. Chem. Soc.* **1978**, *100*, 6128. (c) Wilbur, J. L.; Brauman, J. I. *J. Am. Chem. Soc.* **1994**, *116*, 12125. (d) DePuy, C. H.; Grabowski, J. J.; Bierbaum, V. M.; Ingemann, S.; Nibbering, N. M. M. *J. Am. Chem. Soc.* **1985**, *107*, 1093. (e) Bernasconi, C. F.; Stronach, M. W.; DePuy, C. H.; Gronert, S. *J. Am. Chem. Soc.* **1990**, *112*, 9044. (f) Frink, B. T.; Hadad, C. M. *J. Chem. Soc., Perkin Trans. 2* **1999**, 2397. (g) van der Wel, H.; Nibbering, N. M. M. *Recl. Trav. Chim. Pays-Bas* **1988**, *107*, 479.

(6) Blair, L. K.; Isolani, P. C.; Riveros, J. M. *J. Am. Chem. Soc.* **1973**, *95*, 1057.

(7) Faigle, J. F. G.; Isolani, P. C.; Riveros, J. M. *J. Am. Chem. Soc.* **1976**, *98*, 2049.

(8) van der Wel, H.; Nibbering, N. M. M. *Int. J. Mass Spectrom. Ion Processes* **1986**, *72*, 145.

(9) Johlman, C. L.; Wilkins, C. L. *J. Am. Chem. Soc.* **1985**, *107*, 327.

(10) Reaction 1a has been informally referred to in gas-phase ion chemistry as the "Riveros reaction".

(11) Takashima, K.; Riveros, J. M. *Mass Spectrom. Rev.* **1998**, *17*, 409.

(12) (a) Larson, J. W.; McMahon, T. B. *J. Am. Chem. Soc.* **1983**, *105*, 2944. (b) Caldwell, G.; Rozeboom, M. D.; Kiplinger, J. P.; Bartmess, J. E. *J. Am. Chem. Soc.* **1984**, *106*, 4660−4667. (c) Chabinyc, M. L.; Brauman, J. I. *J. Am. Chem. Soc.* **1998**, *120*, 10863.

(13) (a) Chabinyc, M. L.; Brauman, J. I. *J. Am. Chem. Soc.* **2000**, *122*, 8739. (b) Baer, S.; Brauman, J. I. *J. Am. Chem. Soc.* **1992**, *114*, 5733. (c) Dodd, J. A.; Baer, S.; Moylan, C. R.; Brauman, J. I. *J. Am. Chem. Soc.* **1991**, *113*, 5942. (d) Lim, K. F.; Brauman, J. I. *J. Chem. Phys.* **1991**, *95*, 7164.

(14) (a) Yang, Y.; Linnert, H. V.; Riveros, J. M.; Williams, K. R.; Eyler, J. R. *J. Phys. Chem. A* **1997**, *101*, 2371. (b) Peiris, D. M.; Riveros, J. M.; Eyler, J. R. *Int. J. Mass Spectrom. Ion Processes* **1996**, *159*, 169. (c) Mihalick, J. E.; Gatev, G. G.; Brauman, J. I. *J. Am. Chem. Soc.* **1996**, *118*, 12424.

(15) Pliego, J. R., Jr.; Riveros, J. M. *Chem. Eur. J.* **2001**, *7*, 169.

(16) Isolani, P. C.; Riveros, J. M. *Chem. Phys. Lett.* **1975**, *33*, 361.

(17) (a) Silva, M. L. P.; Riveros, J. M. *J. Mass Spectrom.* **1995**, *30*, 733. (b) Morgon, N. H.; Argenton, A. B.; Silva, M. L. P.; Riveros, J. M. *J. Am. Chem. Soc.* **1997**, *119*, 1708. (c) Morgon, N. H.; Xavier, L. A.; Riveros, J. M. *Int. J. Mass Spectrom.* **2000**, *195*, 363. (d) Moraes, P. R. P.; Linnert, H. V.; Aschi, M.; Riveros, J. M. *J. Am. Chem. Soc.* **2000**, *122*, 10133.

(18) This methodology has been shown to yield reliable kinetic data. For some recent examples, see (a) Nixdorf, A.; Grützmacher, H. F. *Chem. Eur. J.* **2001**, *7*, 1248. (b) Büchner, M.; Grützmacher, H. F. *Int. J. Mass Spectrom.* **2000**, *199*, 141. (c) Nixdorf, A.; Grützmacher, H. F. *Int. J. Mass Spectrom.* **2000**, *195*/*196*, 533.

(19) McIver, R. T.; Hunter, R. L.; Baykutt, G. *Anal. Chem.* **1989**, *61*, 491.

(20) For some of the merits of impulse excitation, see Uechi, G. T.; Dunbar, R. C. *J. Am. Soc. Mass Spectrom.* **1992**, *3*, 734.

(21) For problems associated with quantitation of ionic products under chirp excitation, see, (a) Rempel, D. L.; Huang, S. K.; Gross, M. *Int. J. Mass Spectrom. Ion Processes* **1986**, *70*, 163. (b) Moini, M.; Eyler, J. R. *Int. J. Mass Spectrom. Ion Processes* **1989**, *87*, 29.

(22) Baer, S.; Stoutland, P. O.; Brauman, J. I. *J. Am. Chem. Soc.* **1989**, *111*, 4097.

(23) Frisch, M. J.; Trucks, G. W.; Schlegel, H. B.; Gill, P. M. W.; Johnson, B. G.; Robb, M. A.; Cheeseman, J. R.; Keith, T.; Petersson, G. A.; Montgomery, J. A.; Raghavachari, K.; Al-Laham, M. A.; Zakrzewski, V. G.; Ortiz, J. V.; Foresman, J. B.; Cioslowski, J.; Stefanov, B. B.; Nanayakkara, A.; Challacombe, M.; Peng, C. Y.; Ayala, P. Y.; Chen, W.; Wong, M. W.; Andres, J. L.; Replogle, E. S.; Gomperts, R.; Martin, R. L.; Fox, D. J.; Binkley, J. S.; Defrees, D. J.; Baker, J.; Stewart, J. P.; Head-Gordon, M.; Gonzalez, C.; Pople, J. A. *Gaussian 94*, Version D.2, Revision D.2; Gaussian, Inc.: Pittsburgh, PA, 1994.

(24) *NIST Chemistry WebBook, NIST Standard Reference Database Number 69*; Mallard, W. G., Lindstrom, P. J., Eds.; NIST: Gaithersburg, MD, 2000; (http://webbook.nist.gov/chemistry/).

(25) Zhan, C.-G.; Landry, D. W.; Ornstein, R. L. *J. Am. Chem. Soc.* **2000**, *122*, 1522.

(26) The barrier of this step is sensitive to the size of the basis set and the level of correlation energy included in the calculation. In fact, as reported in ref 5f, calculations at the B3LYP/6-31+G* level predict this step to involve a barrier that is slightly above the energy of the reagent molecules!

(27) Wladkowski, B. D.; East, A. L. L.; Mihalick, J. E.; Allen, W. D.; Brauman, J. I. *J. Chem. Phys.* **1994**, *100*, 2058.

(28) Zhu, L.; Hase, W. L. *A General RRKM Program*; Department of Chemistry, Wayne State University, 1993.

(29) Calculations were performed up to 10 kcal mol^{-1} of excess energy.

(30) This calculation is based on the revised binding energy for the chloride ion−methanol adduct as reported by Bogdanov, B.; Peschke, M.; Tonner, D. S.; Szulejko, J. E.; McMahon, T. B. *Int. J. Mass Spectrom.* **1999**, *185*/*186*/*187*, 707.

(31) (a) Riveros, J. M.; Breda, A. C.; Blair, L. K. *J. Am. Chem. Soc.* **1973**, *95*, 4066. (b) Riveros, J. M.; Jose, S. M.; Takashima, K. *Adv. Phys. Org. Chem.* **1985**, *21*, 197.

(32) Blake, J. F.; Jorgensen, W. L. *J. Am. Chem. Soc.* **1987**, *109*, 3856.

(33) (a) Asubiojo, O. I.; Brauman, J. I. *J. Am. Chem. Soc.* **1979**, *101*, 3715. (b) Wilbur, J. L.; Brauman, J. I. *J. Am. Chem. Soc.* **1994**, *116*, 5839.